Society of Medical Education & Research

2023, Volume 3, Issue 2, Page No: 100-119
ISSN: 3108-4834

Archive of International Journal of Cancer and Allied Science

Overexpression of USP36 stabilizes RBM28 via deubiquitination, leading to p53 suppression and poor prognosis in colorectal cancer

Dimitra Sofia Georgiou[1]*, Ioanna Maria Karagianni[1]

[1]Department of Radiation Oncology, Aristotle University of Thessaloniki, Thessaloniki, Greece.

***E-mail** ✉ d.georgiou.auth@gmail.com

Abstract

Colorectal cancer (CRC) is the second leading cause of cancer-related deaths worldwide, and the tumor suppressor p53 has a crucial role in CRC progression. Ubiquitin-specific protease 36 (USP36), a member of the deubiquitinating enzyme family, contributes to tumor development in various cancers. However, the mechanisms through which USP36 influences the p53 signaling pathway in CRC are not fully understood. In this study, we observed that USP36 expression was elevated in CRC tissues and correlated with worse clinical outcomes. Functionally, high USP36 enhanced CRC cell growth, migration, and invasion in both in vitro and in vivo models. Mechanistically, USP36 interacted with RBM28 and stabilized it via deubiquitination at the K162 residue. In turn, increased RBM28 inhibited p53 transcriptional activity, suppressing the p53 signaling pathway. Collectively, our results reveal a previously unrecognized USP36/RBM28/p53 axis that promotes CRC progression and may represent a potential therapeutic target.

Keywords: Colorectal cancer, Prognostic markers, cancer, Tumor development

Introduction

Colorectal cancer (CRC) is among the most prevalent malignancies worldwide and ranks second in terms of mortality [1]. Despite the emergence of treatments such as neoadjuvant chemoradiotherapy and immunotherapy, CRC patients often face poor survival outcomes [2, 3]. Therefore, a deeper understanding of the molecular mechanisms underlying CRC development is urgently needed.

The ubiquitin-proteasome system, a critical post-translational modification pathway, controls protein degradation through ubiquitination [4, 5]. Evidence indicates that dysregulated ubiquitination contributes to processes like tumor cell proliferation and metastasis [6–9]. This pathway relies on three types of enzymes—E1, E2, and E3 ligases—which attach ubiquitin to proteins [10]. Deubiquitinating enzymes (DUBs) reverse this process by removing ubiquitin, counteracting E3 ligase activity [11, 12]. Currently, nearly 100 DUBs are classified into six families: USPs, UCHs, OTUs, JAMM, MCPIPs, and MINDYs [13]. USP36, a USP family member, is aberrantly expressed in multiple cancers and regulates substrates via deubiquitination. For instance, USP36 stabilizes ALKBH5 in glioblastoma [14], promotes Hippo signaling by stabilizing TAZ and YAP in gastric cancer and ESCC [15, 16], and accelerates HCC progression by inhibiting MDM2 [17]. Nevertheless, its molecular role in CRC remains unclear. p53, a key transcription factor and tumor suppressor, regulates diverse cellular processes including apoptosis, cell cycle, senescence, metastasis, and metabolism [18–20]. Its anti-tumor activity primarily occurs through transcriptional regulation of genes such as CDKN1A, BAX, and FAS [21, 22]. However, the lack of

Access this article online https://smerpub.com/

Received: 23 April 2023; **Accepted:** 05 September 2023

How to cite this article: Georgiou DS, Karagianni IM. Overexpression of USP36 stabilizes RBM28 via deubiquitination, leading to p53 suppression and poor prognosis in colorectal cancer. Arch Int J Cancer Allied Sci. 2023;3(2):100-19. https://doi.org/10.51847/CG7lUfVB1v

conventional druggable features limits p53-targeted therapy [23]. Identifying negative regulators of p53 may provide alternative strategies for cancer treatment.

RBM28, an RNA-binding protein within spliceosomal small nuclear ribonucleoproteins (snRNPs), plays a role in the nucleolar stress response. RBM28 is enriched in platelet RNAs of lung cancer [24] and linked to splicing changes in head and neck and lung squamous cell carcinomas [25]. Importantly, RBM28 can bind p53's DNA-binding domain, suppressing its transcriptional function [26]. Its regulatory role in CRC, however, is not fully characterized.

In this study, we demonstrate that USP36 is upregulated in CRC and correlates with poor prognosis. Mechanistically, USP36 stabilizes RBM28 through K162 deubiquitination, which subsequently inhibits the p53 pathway. These findings uncover a novel USP36-RBM28-p53 axis and suggest a potential therapeutic avenue for CRC treatment.

Results and Discussion

USP36 suppresses the p53 pathway by reducing p53-mediated gene transcription

To explore the involvement of USP36 in colorectal cancer (CRC) advancement, initial examination of the TCGA database showed marked elevation of USP36 in CRC specimens [1]. Additionally, evaluation of publicly available datasets such as GEO (GSE100179, GSE41258) and gene array information indicated higher USP36 levels in adenomas, primary tumors, and metastatic sites compared to nearby healthy tissue [1]. Furthermore, Kaplan-Meier survival curves from the GEO dataset (GSE40967) demonstrated that elevated USP36 correlated with shorter relapse-free and overall survival [1]. Gene set enrichment analysis (GSEA) performed on TCGA data was then used to identify signaling pathways linked to USP36 in CRC. Enrichment plots revealed a clear negative association between USP36 and the p53 pathway **(Figure 1a)** [1]. This prompted further examination of whether USP36 directly influences p53 pathway activity.

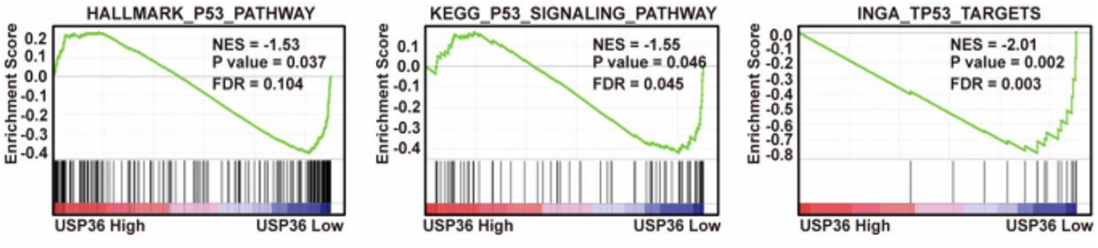

a)

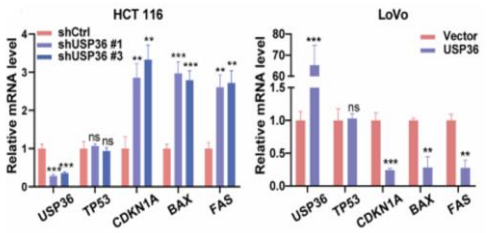

b)

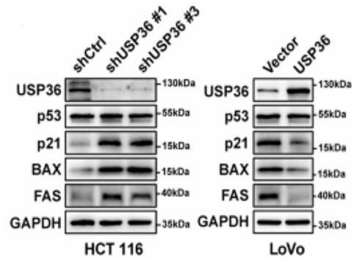

c)

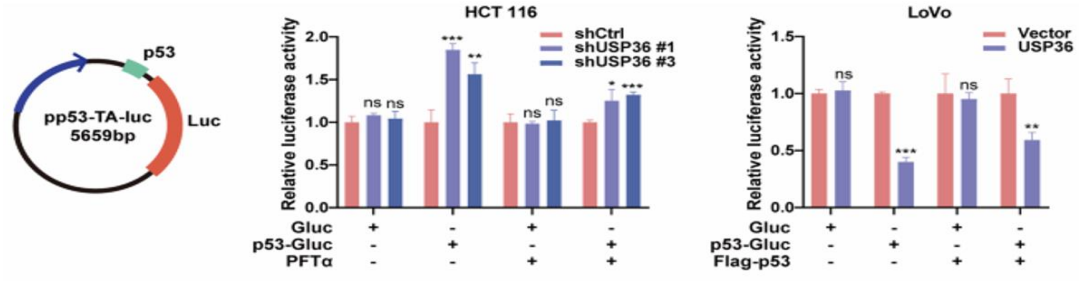

d)

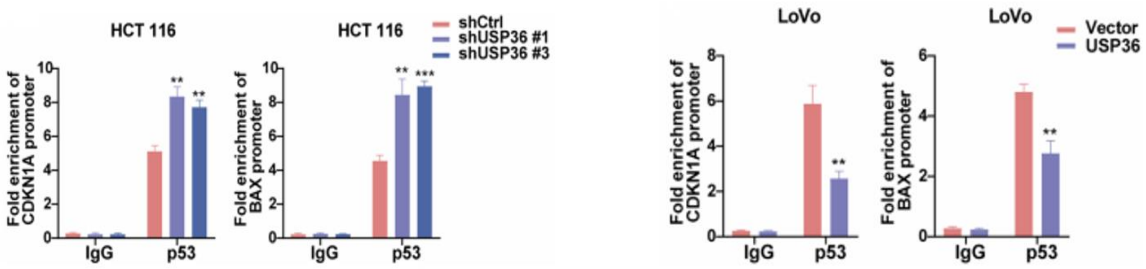

e) f)

Figure 1. USP36 blocks p53 pathway activation through reduction of p53 transcriptional function.

A GSEA results illustrating the negative relationship between USP36 expression and p53 pathway in TCGA-derived data. NES: normalized enrichment score. FDR: false discovery rate. B, C Changes in mRNA and protein amounts of p53 along with its downstream targets in CRC cell lines following USP36 depletion or forced expression. D Luciferase-based reporter experiments showed that USP36 knockdown strongly enhanced p53 activity, an effect abolished by the p53 blocker pifithrin-α (left). Overexpression of p53 reversed the USP36-driven suppression of p53 transcription (right). E, F ChIP-qPCR analysis assessing p53 occupancy on CDKN1A and BAX promoters in CRC cells after USP36 knockdown or overexpression. Data represent means ± SD from three separate experiments. *$p < 0.05$, **$p < 0.01$, ***$p < 0.001$, ns: not significant [1].

Stable CRC cell lines were generated using lentiviral delivery of shCtrl, shUSP36 #1/#2/#3, empty vector, or USP36-expressing constructs. Knockdown validation favored shUSP36 #1 and #3 for subsequent work due to their stronger silencing efficiency over #2 **(figures. 5a and 5b)** [5]. USP36 reduction in HCT 116 and RKO lines increased both mRNA and protein levels of p53 downstream targets, whereas USP36 elevation in LoVo cells produced the opposite outcome **(Figures 1b and 1c)** [1]. Notably, p53 itself showed no change in expression with USP36 manipulation. Luciferase assays confirmed enhanced p53-driven transcription upon USP36 silencing in HCT 116 and RKO cells, reversible by pifithrin-α (PFT-α) treatment **(Figure 1d)** [1]. Conversely, excess p53 countered the transcriptional repression caused by USP36 overexpression in LoVo cells **(Figure 1d)** [1]. ChIP experiments further demonstrated strengthened p53 binding to promoters of classic targets like p21 and BAX after USP36 loss, with reduced binding upon USP36 gain **(Figures 1e and 1f)** [1]. Together, these data establish that USP36 impairs p53 transcriptional function and thereby downregulates the p53 signaling cascade.

USP36 binds to RBM28 and enhances its stability through deubiquitinase function

To uncover how USP36 mediates p53 pathway suppression, mass spectrometry following immunoprecipitation (IP-MS) was employed to detect proteins associating with USP36. Among the leading candidates in the USP36 interactome [2], RBM28 ranked highest in abundance and had prior links to p53 transcription inhibition, making it a prime candidate for USP36 action on p53. Confocal immunofluorescence revealed nuclear co-occurrence of USP36 and RBM28 in HCT 116 and HEK293T cells **(Figure 2a)** [2]. Co-immunoprecipitation in HEK293T and CRC lines confirmed mutual pull-down of tagged USP36 and RBM28 **(Figure 2b)** [2]. Endogenous binding between the two proteins was also verified in CRC cells **(Figure 2c)** [2]. In vitro GST pull-down confirmed direct physical association **(Figure 2d)** [2]. Domain mapping using deletion mutants identified the USP domain of USP36 as critical for RBM28 binding **(Figure 2e)** [2], while the RRM2 region of RBM28 was required for USP36 interaction **(Figure 2f)** [2]. These observations firmly support a direct protein-protein interaction between USP36 and RBM28.

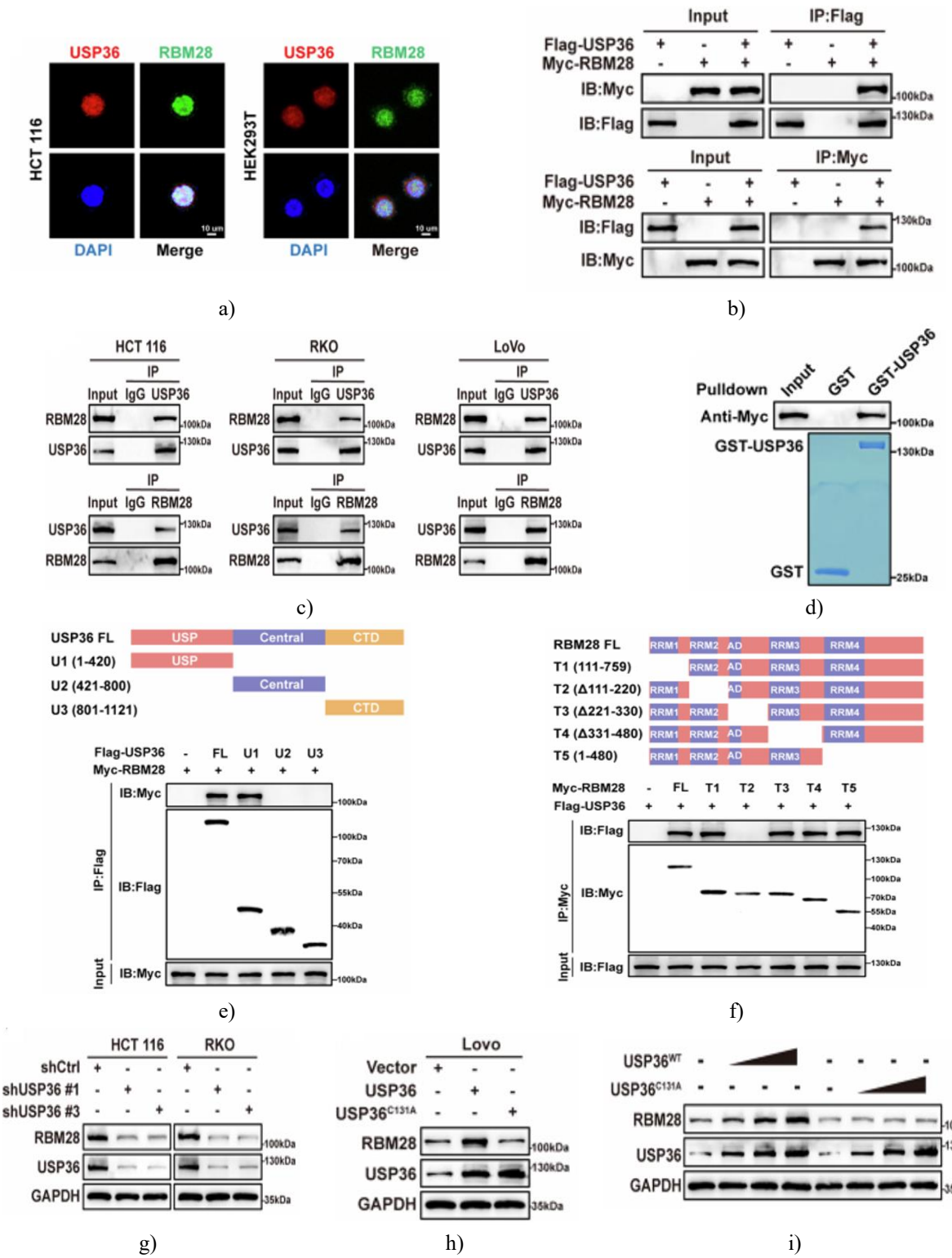

Figure 2. USP36 binds to RBM28 and enhances its levels via deubiquitinase function.

A Cells from HCT 116 and HEK293T lines were prepared, fixed, and labeled using antibodies against USP36 (red) and RBM28 (green). Nuclear staining was achieved with DAPI (blue). Scale bars represent 10 µm. B HEK293T cells expressing Flag-tagged USP36 and Myc-tagged RBM28 were collected to confirm

exogenous binding through co-immunoprecipitation and immunoblotting. C Lysates prepared from HCT 116, RKO, and LoVo cells underwent immunoprecipitation using control IgG or antibodies specific to USP36 and RBM28, then analyzed by immunoblot. D Lysates from HEK293T cells expressing Myc-RBM28 were mixed with GST-fused USP36 or GST alone. Bound RBM28 was identified via immunoblotting. E Diagram illustrating USP36 domains and deletion constructs (top). HEK293T cells received Myc-RBM28 together with Flag-USP36 or its truncated forms; lysates were subjected to immunoprecipitation using anti-Flag followed by detection (bottom). F Diagram showing RBM28 domains and mutants (top). HEK293T cells were transfected with Flag-USP36 plus Myc-RBM28 or its deletions; immunoprecipitation was performed with anti-Myc and subsequent immunoblotting (bottom). G Immunoblot analysis of RBM28 amounts in HCT116 and RKO cells after introduction of specified shRNAs. H Immunoblot evaluation of RBM28 in LoVo cells expressing either wild-type USP36 or the catalytically inactive C131A variant. I LoVo cells received escalating doses of USP36WT or USP36C131A for 48 h, followed by lysate immunoblotting [2].

Subsequently, the influence of USP36 on RBM28 abundance was examined. Reduction of USP36 caused lowered RBM28 protein in HCT 116 and RKO lines **(Figure 2g)** [2]. In agreement, wild-type USP36 elevated RBM28 protein dose-dependently, while the inactive C131A mutant (USP36C131A) had minimal effect **(Figures 2h and i)** [2]. No alterations in RBM28 mRNA occurred with USP36 manipulation, pointing to post-transcriptional control [2]. Overall, these data show USP36 controls RBM28 levels reliant on its deubiquitinating enzyme activity.

USP36 protects RBM28 from degradation by removing ubiquitin at lysine 162

To determine if USP36 affects RBM28 via proteasomal routes, CRC cells with reduced USP36 were treated with the inhibitor MG132. Results indicated MG132 restored RBM28 protein diminished by USP36 loss **(Figure 3a)** [3]. Cycloheximide chase experiments revealed accelerated RBM28 turnover upon USP36 depletion **(Figure 3b)** [3]. Conversely, forced expression of wild-type USP36, unlike the C131A mutant, extended RBM28 stability **(Figure 3b)** [3]. These observations confirm that USP36 maintains RBM28 by blocking proteasome-mediated breakdown.

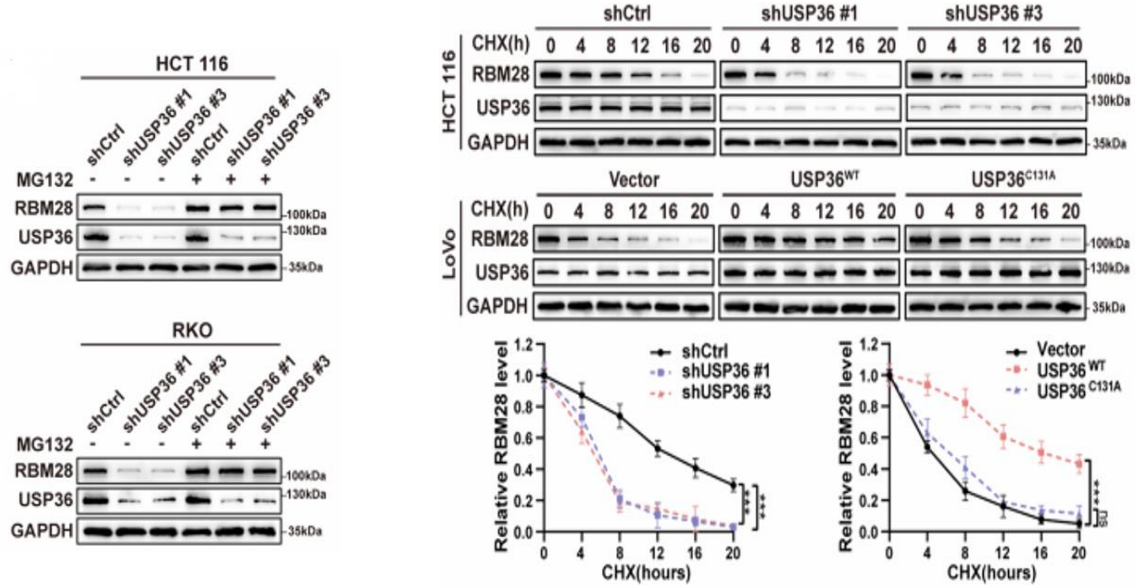

a) b)

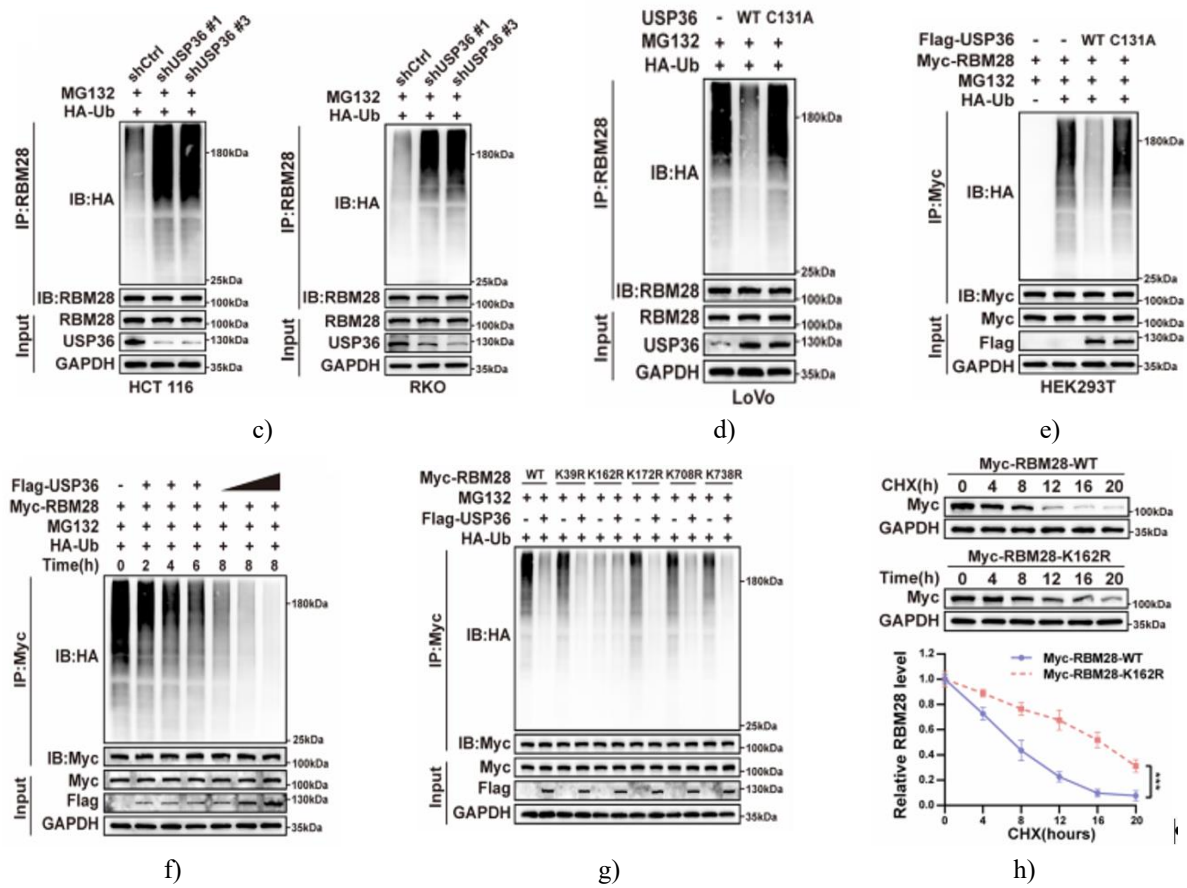

c) d) e)

f) g) h)

Figure 3. USP36 maintains RBM28 stability and performs deubiquitination at the lysine 162 site.

A HCT 116 and RKO cells subjected to USP36 knockdown were exposed to vehicle or the proteasome blocker MG132 (10 μM, 6 h), followed by protein extraction and detection. B Turnover assessment of RBM28 in HCT 116-shUSP36 #1/3 cells, LoVo-USP36WT cells, and LoVo-USP36C131A cells after treatment with 10 μg/mL cycloheximide (CHX) across specified durations. Lower sections display densitometric quantification of RBM28 bands. C USP36-reduced HCT 116 and RKO cells received 10 μM MG132 for 6 h prior to collection. Anti-RBM28 antibody was used for pull-down, with HA antibody for ubiquitin probing on immunoblots. D LoVo cells expressing designated constructs underwent 10 μM MG132 treatment for 6 h, then sequential immunoprecipitation and immunoblot examination. E Ubiquitination of RBM28 was evaluated by immunoblot in HEK293T cells co-expressing Myc-RBM28, HA-Ubiquitin, and Flag-USP36 (wild-type or C131A variant), following 10 μM MG132 exposure for 6 h. F USP36 cleaved ubiquitin chains from RBM28 dependent on both duration and concentration. G Ubiquitination patterns of RBM28 variants were examined via immunoblot in HEK293T cells co-transfected with Myc-tagged mutant RBM28, Flag-USP36, and HA-Ub; 10 μM MG132 applied for 6 h before harvest. H HEK293T cells carrying Myc-RBM28-WT or Myc-RBM28-K162R were administered 10 μg/mL CHX for designated periods, followed by immunoblot analysis. Lower section provides quantification of wild-type versus K162R RBM28 amounts. All results represent means ± SD across three separate replicates. ***$p < 0.001$ [3].

Given USP36's classification as a deubiquitinase, we investigated its capacity to remove ubiquitin from RBM28. Reducing USP36 substantially elevated native RBM28 ubiquitination in HCT 116 and RKO lines **(Figure 3C)** [3]. On the contrary, forced expression of wild-type USP36, unlike the inactive C131A form, strongly lowered RBM28 ubiquitination in LoVo and HEK293T cells **(Figures 3d and 3e)** [3]. In-cell ubiquitination tests further confirmed time- and dose-reliant ubiquitin removal from RBM28 by USP36

(Figure 3f) [3]. As K29-, K48-, and K63-linked chains often govern protein lifespan, we determined the chain type targeted by USP36 on RBM28. Results from deubiquitination experiments indicated predominant cleavage of K48 linkages [3].

To pinpoint the precise lysine(s) on RBM28 affected by USP36, five candidate sites were identified via computational prediction tools. Site-directed mutants were generated by replacing each lysine with arginine. Data revealed that USP36 failed to alter ubiquitination of the K162R variant, yet markedly reduced it for wild-type RBM28 and the remaining mutants (K39R, K172R, K708R, K738R) **(Figure. 3*g*)** [3]. Moreover, the K162R substitution prolonged RBM28 half-life compared to the wild-type protein **(Figure 3h)** [3]. These observations confirm that USP36 enhances RBM28 stability specifically by deubiquitinating the K162 position.

RBM28 mediates USP36-driven suppression of p53 transcriptional function

Prior evidence showed RBM28 attachment to p53's DNA-binding domain, thereby blocking p53-dependent gene activation [26]. In light of USP36's role in RBM28 stabilization, we tested if USP36 disrupts p53 signaling through RBM28. Consistent with expectation, gene set enrichment analysis of TCGA colorectal cancer data revealed an inverse relationship between RBM28 and p53 pathway activity **(Figure 4a)** [4]. Co-immunoprecipitation verified RBM28-p53 association within colorectal cancer cells **(Figure 4b)** [4]. Immunofluorescence further confirmed overlapping nuclear distribution of RBM28 and p53 in these cells **(Figure 4c)** [4]. Elevating RBM28 substantially lowered mRNA and protein amounts of p53 downstream targets, whereas RBM28 reduction produced opposing increases **(Figures. 4d and 4e)** [4]. Reporter gene assays indicated reduced p53-driven transcription with RBM28 gain and heightened activity with RBM28 loss **(Figure. 4f)** [4]. Chromatin immunoprecipitation demonstrated diminished p53 recruitment to target promoters upon RBM28 overexpression and enhanced recruitment after depletion **(Figure. 4g and 4h)** [4]. In aggregate, these results establish that BM28 physically associates with p53 and impairs its gene-regulatory capacity.

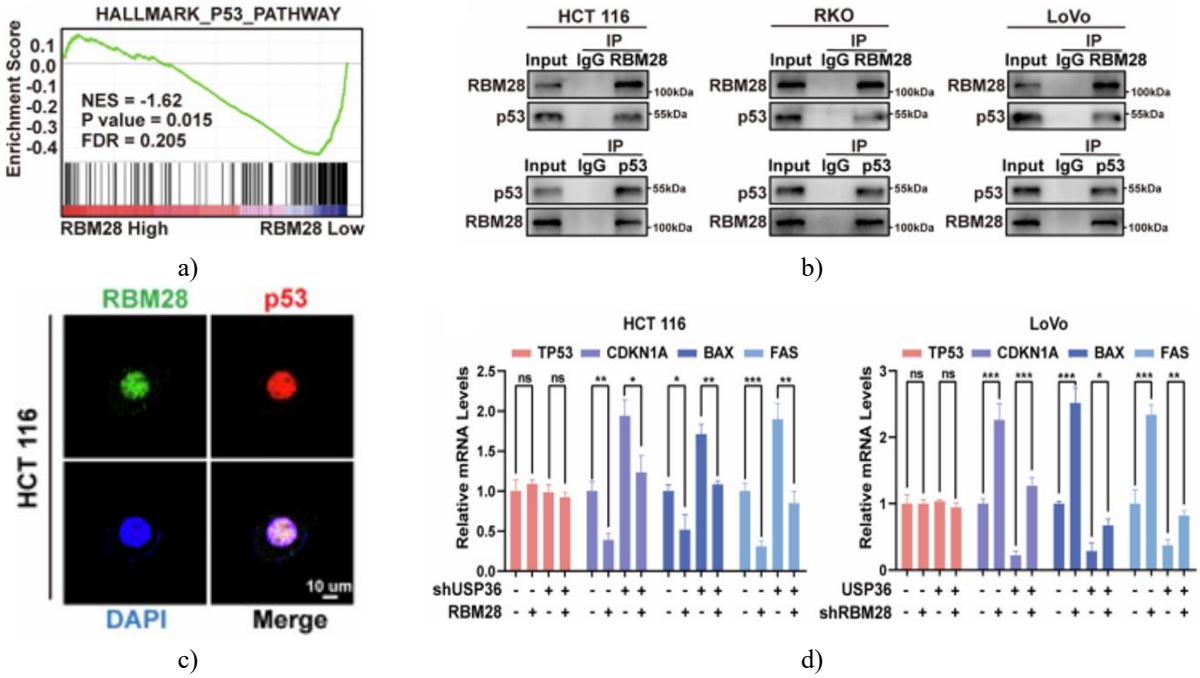

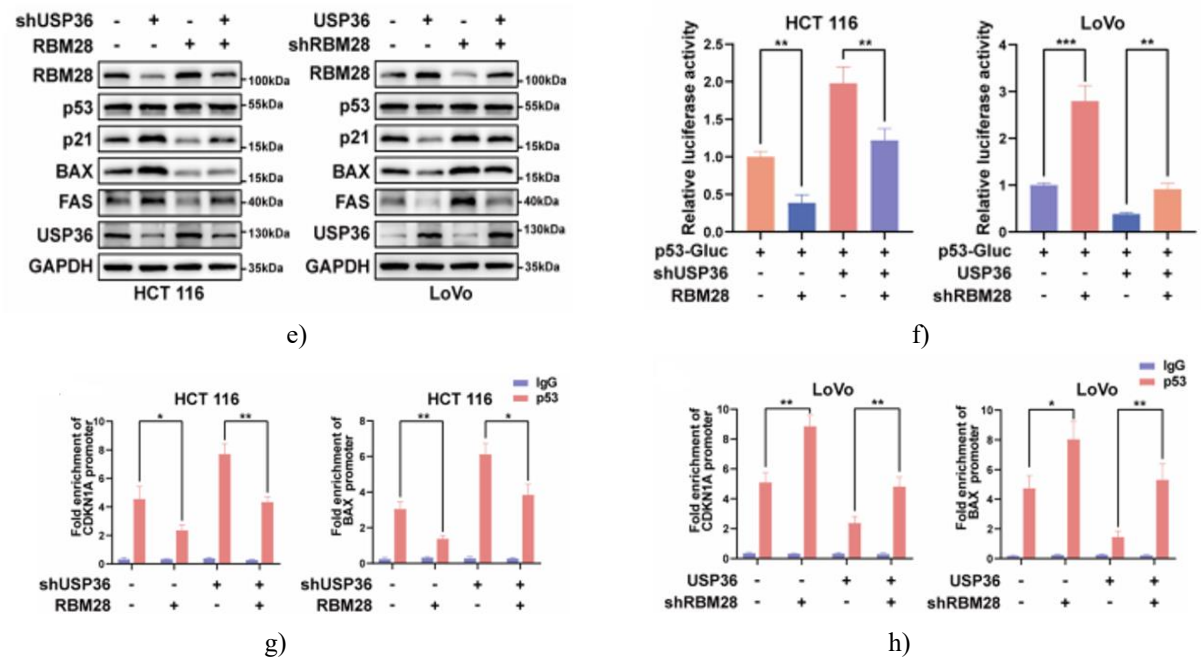

Figure 4. RBM28 is essential for USP36-driven suppression of p53 transcriptional function**.**

(a) Gene set enrichment analysis (GSEA) showing the association between RBM28 expression and p53 signaling based on TCGA datasets. ES, normalized enrichment score; FDR, false discovery rate.

(b) Co-immunoprecipitation (Co-IP) demonstrating the endogenous interaction between RBM28 and p53 in CRC cells. Lysates from HCT 116, RKO, and LoVo cells were immunoprecipitated using IgG, anti-p53, or anti-RBM28 antibodies, followed by western blot analysis. Input lysates are shown.

(c) Immunofluorescence assays illustrating the nuclear co-localization of RBM28 (green) and p53 (red) in HCT 116 cells. Nuclei were stained with DAPI (blue). Scale bars, 10 μm.

(d, e) In HCT 116-shUSP36 cells and LoVo-USP36-overexpressing cells, RBM28 levels were modulated via lentiviral transduction or shRNA, and the expression of p53 and its downstream targets was quantified by qRT-PCR and western blotting.

(f) Luciferase reporter assays measuring p53 pathway activation in the indicated cells.

(g, h) ChIP-qPCR evaluating p53 binding to CDKN1A and BAX promoters in the indicated experimental conditions. Data represent mean ± SD from three independent experiments. *p < 0.05, **p < 0.01, ***p < 0.001, ns, not significant.

Analysis revealed that the elevation of p53 target genes caused by USP36 knockdown was reversed when RBM28 was overexpressed. Conversely, silencing RBM28 in USP36-overexpressing cells restored the expression of these targets to higher levels **(Figures 4d, and 4e)**. Consistently, luciferase reporter assays showed that RBM28 overexpression negated the increase in p53 transcriptional activity induced by USP36 depletion, while RBM28 knockdown suppressed p53 activity in USP36-overexpressing cells **(Figures 4f and 2j).** Moreover, ChIP-qPCR demonstrated that RBM28 overexpression reversed the enhanced binding of p53 to promoters of CDKN1A and BAX triggered by USP36 silencing, whereas RBM28 depletion led to the opposite effect **(Figures. 4g, 4h and 2k).** These results indicate that RBM28 serves as a critical intermediary in USP36-mediated regulation of the p53 pathway.

USP36 promotes proliferation, migration, and invasion of CRC cells in vitro

Considering that USP36 stabilizes RBM28 to inhibit p53 activity, we assessed the functional consequences of USP36 modulation in CRC cells. Cell proliferation assays, including CCK8 and colony formation, demonstrated that USP36 knockdown in HCT 116 and RKO cells markedly reduced cell growth, while USP36 overexpression in LoVo cells enhanced proliferation **(Figures. 5c–f and 3b, 3c).** Flow cytometry revealed that USP36 depletion increased apoptosis in HCT 116 and RKO cells, whereas overexpression decreased apoptosis

in LoVo cells **(Figures. 5g, 5h and 3d).** Furthermore, migration and invasion assays using transwell and wound healing approaches showed that USP36 silencing impaired motility and invasive capacity in HCT 116 and RKO cells, whereas USP36 overexpression promoted these phenotypes **(Figures. 5i–l and 3e, f).** Collectively, these in vitro studies indicate that USP36 facilitates CRC cell proliferation, migration, and invasion.

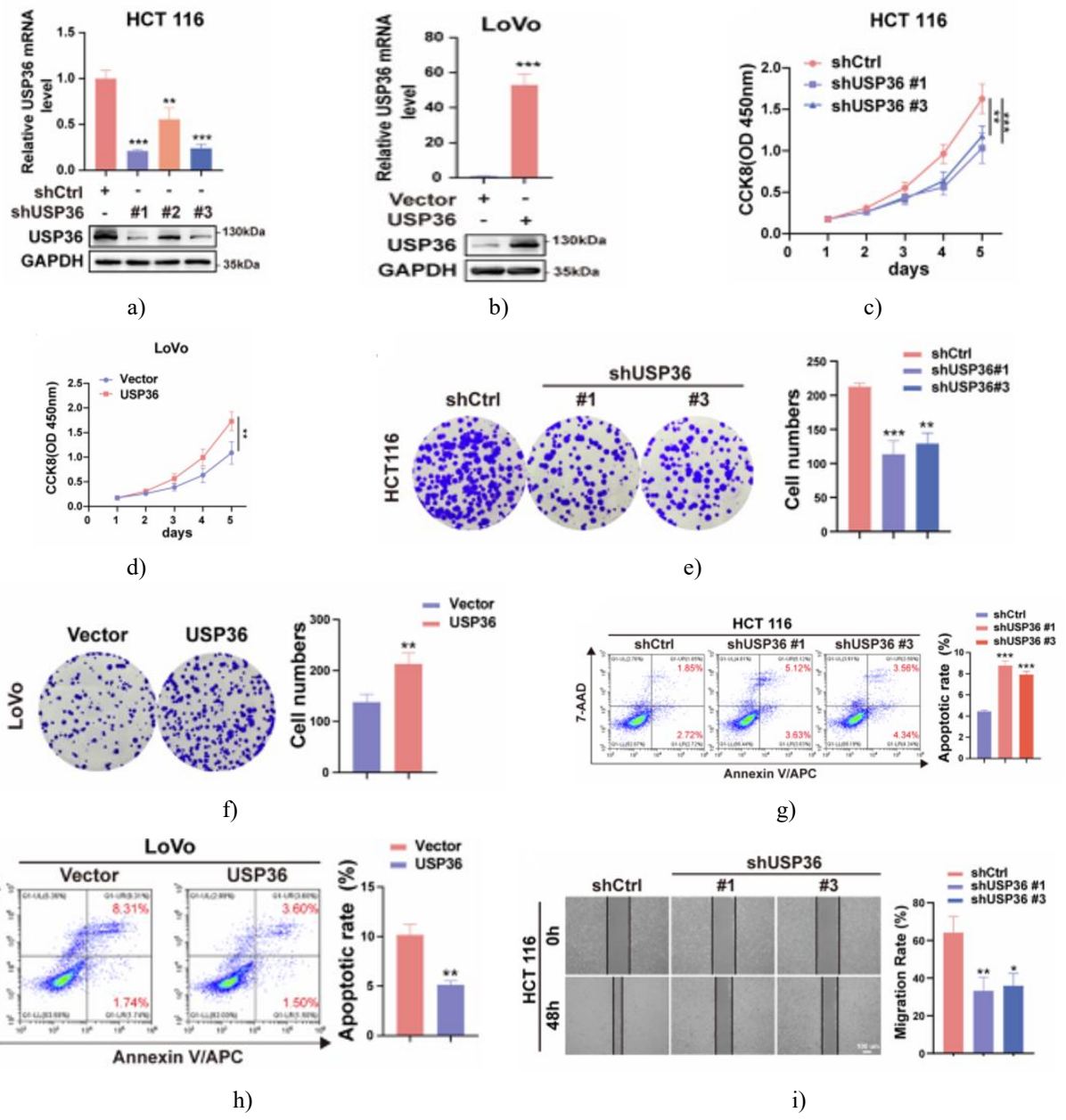

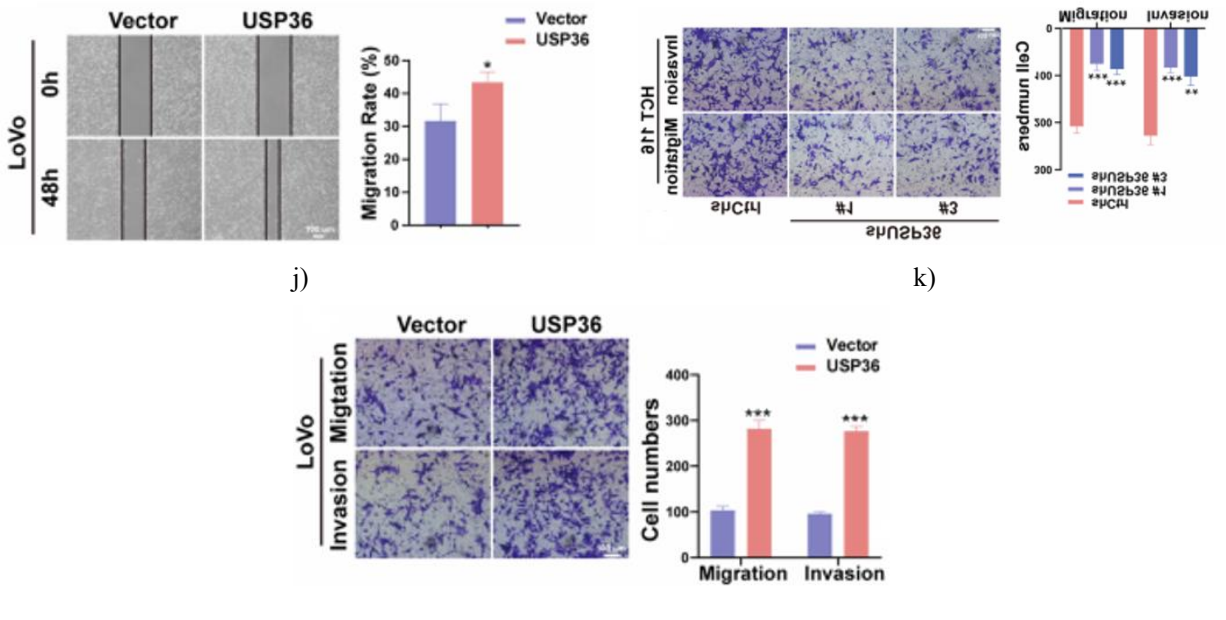

Figure 5. USP36 enhances colorectal cancer cell growth and spread in vitro.

A, B Validation of USP36 manipulation efficiency in HCT 116 and LoVo lines via qRT-PCR and immunoblotting. C, D Cell viability was measured using CCK8 assays in cells with reduced or elevated USP36. E, F Long-term proliferative capacity of CRC cells was assessed through colony formation experiments. G, H Apoptosis percentages (LR + UR) were determined by flow cytometry. LR denotes early-stage apoptosis; UR indicates late-stage apoptosis. I, J Migration potential was evaluated with wound healing experiments. K, L Transwell chambers were employed to quantify migration and invasive properties of CRC cells. All results are shown as means ± SD from three separate experiments. *p < 0.05, **p < 0.01, ***p < 0.001 [5].

USP36 drives colorectal cancer growth and metastatic spread in vivo

To examine the biological role of USP36 in living organisms, the previously described CRC cell lines were utilized to generate subcutaneous xenograft tumors and distant metastasis models. Results indicated that USP36 knockdown produced markedly smaller tumors with significant reductions in both tumor mass and size **(Figure. 6a)** [6]. In contrast, forced USP36 expression yielded the reverse outcomes. Immunohistochemical staining demonstrated lowered Ki67 staining in USP36-deficient tumors and increased Ki67 in those with USP36 overexpression **(Figure 6b)** [6]. Additionally, in models of liver and lung metastasis, the USP36-reduced group displayed diminished bioluminescent signals and fewer metastatic lesions, while USP36-overexpressing cells showed heightened signals and more nodules **(Figures. 6c–f)** [6]. Overall, these data confirm that USP36 actively contributes to colorectal cancer proliferation and metastasis in vivo.

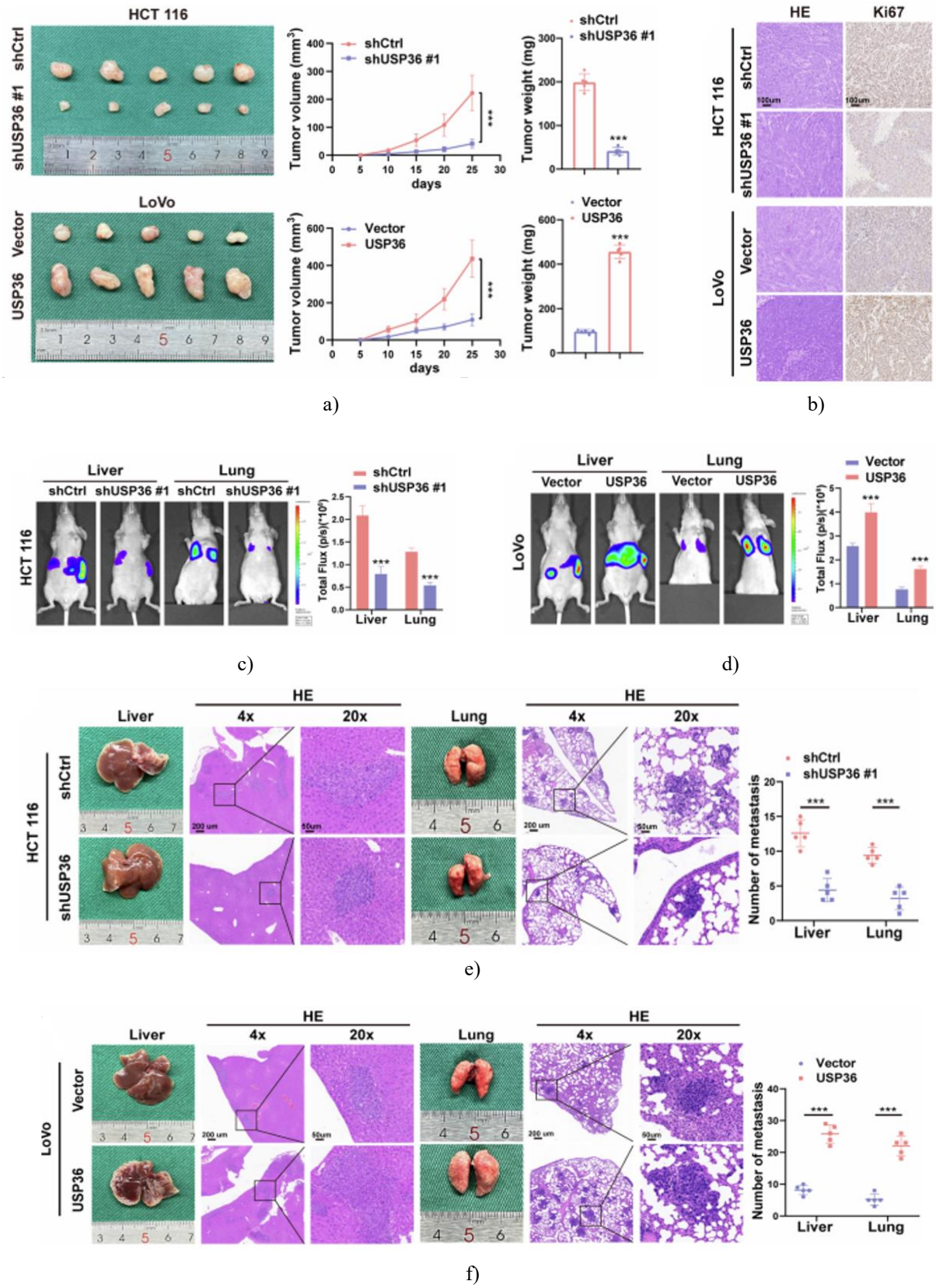

Figure 6. USP36 drives colorectal cancer growth and metastatic spread in vivo.

A Example images of subcutaneous tumors excised from nude mice. Tumor sizes were recorded every 5 days, and final tumor masses were weighed. B Hematoxylin-eosin staining and immunohistochemical detection of Ki67 in xenografts derived from HCT 116 and LoVo cells. C, D Example images and quantification of bioluminescent signals in metastatic models (n = 5 per group). E, F Example photographs and H&E-stained sections of metastatic lesions in mouse livers and lungs. Metastatic nodule counts in liver or lung were quantified. All results are shown as means ± SD from three separate experiments. ***p < 0.001 [6].

USP36 shows positive association with RBM28 in colorectal cancer specimens

To assess the clinical significance of USP36 and RBM28, their protein amounts and relationship were first evaluated in human colorectal cancer tissues using immunoblotting and immunohistochemistry (IHC). Immunoblotting demonstrated markedly higher levels of both USP36 and RBM28 in tumor samples versus adjacent normal tissue **(Figure 7a)** [7], with a clear positive relationship between their expression (n = 24, Pearson R = 0.5165, p = 0.0098) **(Figure 7b)** [7]. IHC on tissue microarrays from 80 matched patient pairs further confirmed this pattern **(Figures 7c and e)** [7]. Scoring of staining intensity revealed significant elevation of both proteins in cancerous regions **(Figures. 7d and f)** [7]. Representative micrographs suggested strong co-expression, supported by Pearson correlation (R = 0.7689, p < 0.0001) **(Figures 7g and h)** [7]. These observations indicate upregulation and mutual positive correlation of USP36 and RBM28 in colorectal cancer.

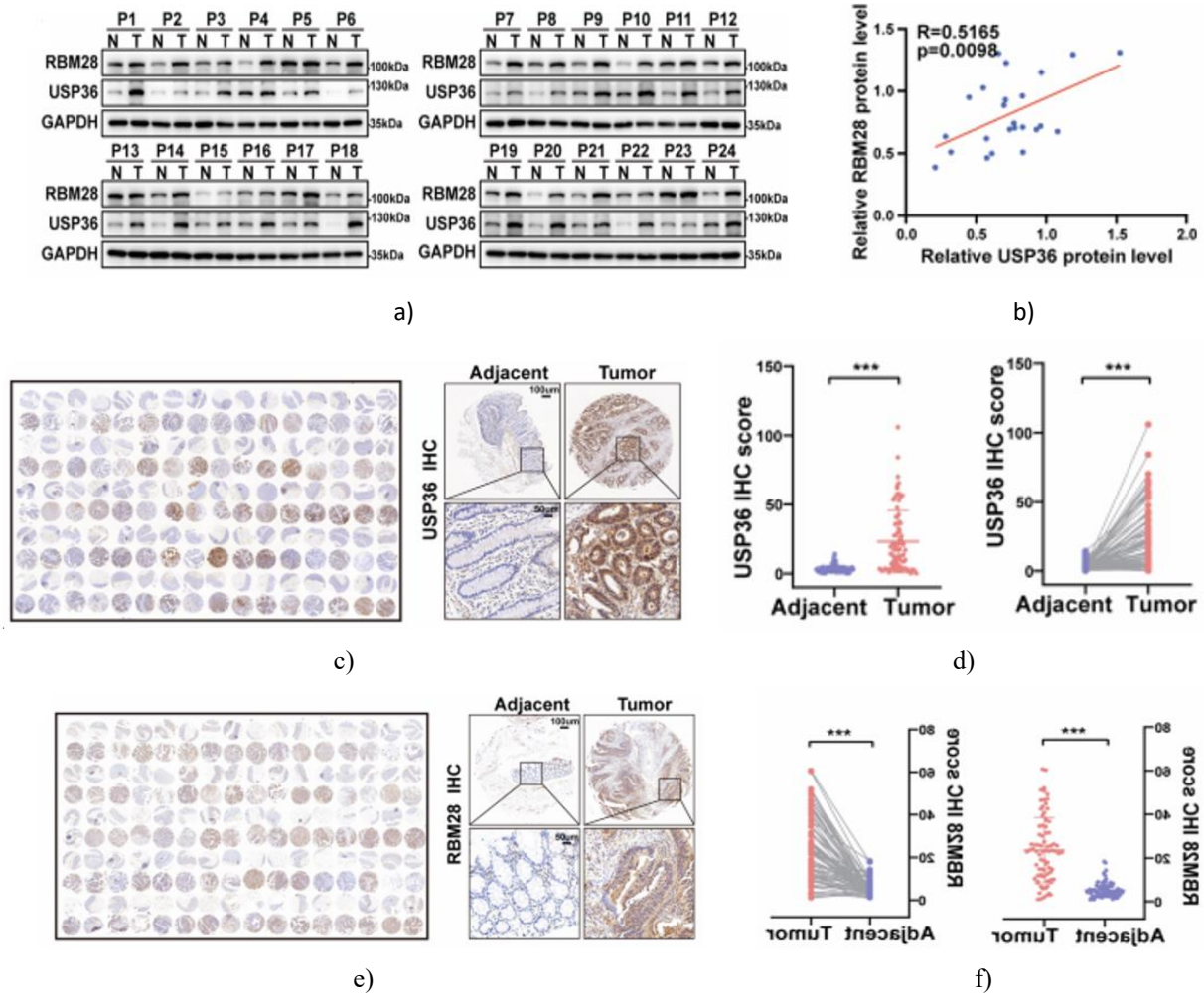

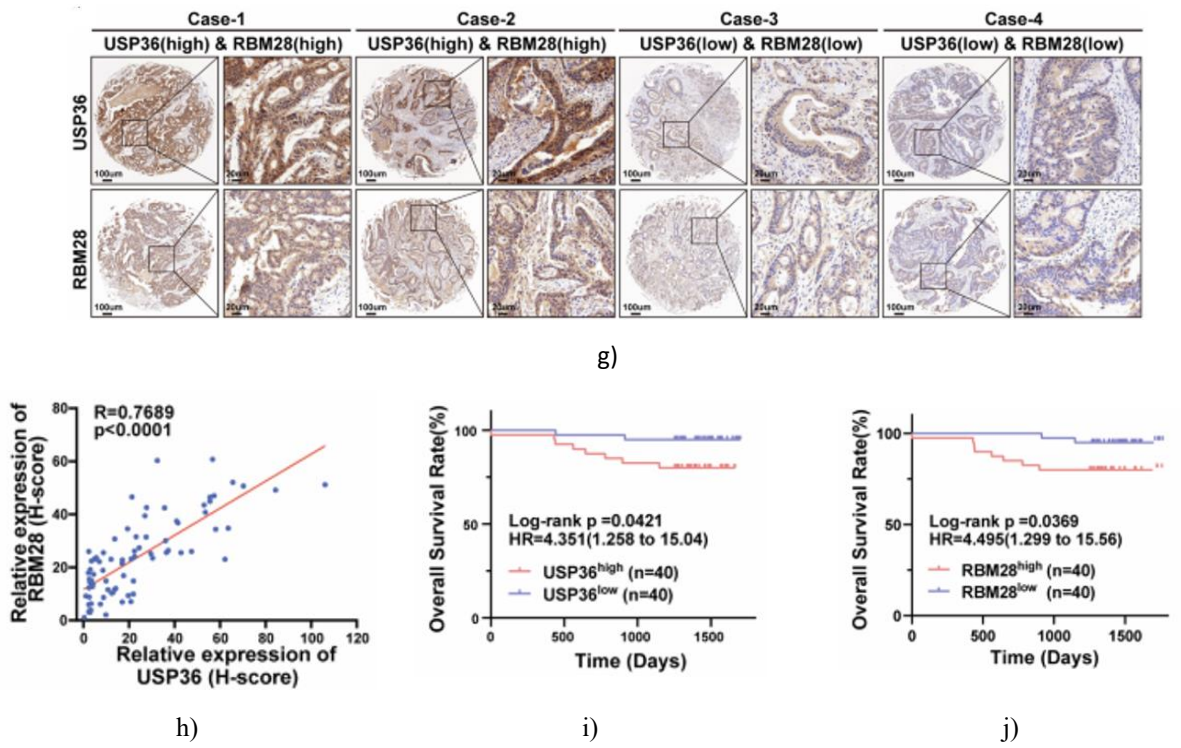

Figure 7. USP36 displays positive correlation with RBM28 in colorectal cancer specimens.

A Immunoblot detection of USP36 and RBM28 in lysates from 24 matched colorectal cancer pairs. B Correlation between USP36 and RBM28 protein amounts in tumor samples (n = 24). Chi-square test was used for statistics. Pearson R denotes correlation coefficient. C, E IHC assessment of USP36 and RBM28 in tissue microarrays from 80 paired patient samples (left). Example images showing strong co-expression in cancer tissue (right). D, F IHC scoring for USP36 and RBM28 across the 80 paired samples. Comparisons used Wilcoxon unpaired test (left) or paired t-test (right). G Example IHC images illustrating concurrent high or low staining for both proteins in patient tissues. H Positive relationship between USP36 IHC scores (X-axis) and RBM28 scores (Y-axis) in colorectal cancer (n = 80). p-value derived from linear regression. R indicates correlation coefficient. I, J Kaplan-Meier curves for overall survival in the 80-patient microarray cohort, stratified by median IHC score into high and low groups for USP36 and RBM28. Log-rank test for p-value. HR: hazard ratio. All results are means ± SD from three independent experiments. ***p < 0.001 [7].

Further analysis linked IHC scores of these proteins to patient clinicopathological features in the microarray cohort. USP36 levels correlated positively with advanced tumor stage (p = 0.0008), lymph node involvement (p = 0.0066), vascular invasion (p = 0.0181), and distant metastasis (p = 0.0026). Similarly, RBM28 associated with tumor stage (p = 0.0136), nodal metastasis (p = 0.0237), vascular invasion (p = 0.0181), and elevated CEA (p = 0.0389). Critically, combined high expression of both proteins showed associations with tumor stage (p = 0.0020), lymph node metastasis (p = 0.0122), vascular invasion (p = 0.0210), distant metastasis (p = 0.0192), and CEA levels (p = 0.0380). Kaplan-Meier survival plots from the microarray indicated reduced overall survival in patients with elevated USP36 or RBM28 compared to low-expression cases **(Figures 7I, J)** [7]. In summary, increased USP36 and RBM28 levels link to worse survival outcomes in colorectal cancer, positioning them as valuable markers for diagnosis and prognostic evaluation.

The RBM28/p53 pathway underlies USP36-driven proliferation and metastasis

To determine if RBM28 mediates the oncogenic effects of USP36, cells with stable USP36 knockdown or control were transduced with RBM28 or empty vector. Conversely, USP36-overexpressing cells received shRBM28 or control lentivirus. In viability and

clonogenic assays, forced RBM28 expression boosted cell growth and rescued the suppression caused by USP36 loss, while RBM28 reduction diminished proliferation and countered the increase from USP36 gain. Apoptosis analysis by flow cytometry showed that extra RBM28 lowered cell death rates and reversed the elevation induced by USP36 silencing, with opposite effects upon RBM28 depletion. Migration and invasion tests indicated that RBM28 elevation strengthened metastatic potential and offset the impairment from USP36 knockdown, and vice versa. In vivo tumor growth experiments confirmed that RBM28 knockdown produced smaller xenografts and abrogated the enhancement driven by USP36, evident in reduced volume, mass, and Ki67 staining (**Figures 8a and b)** [8]. Likewise, metastatic models showed RBM28 silencing decreased liver and lung nodule formation promoted by USP36 overexpression **(Figures 8c–f)** [8]. Overall, these findings establish that USP36 fosters colorectal cancer proliferation and metastasis primarily by stabilizing RBM28.

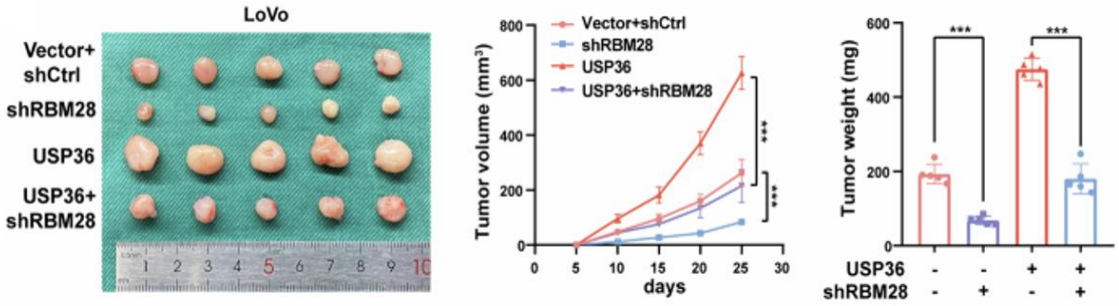

a)

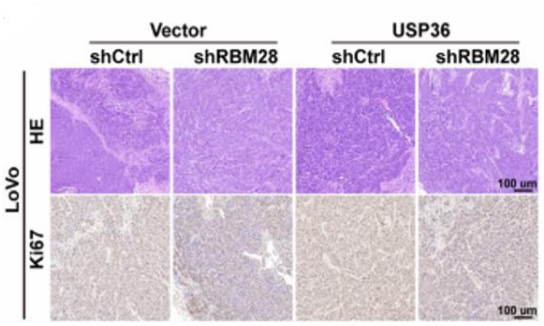

b)

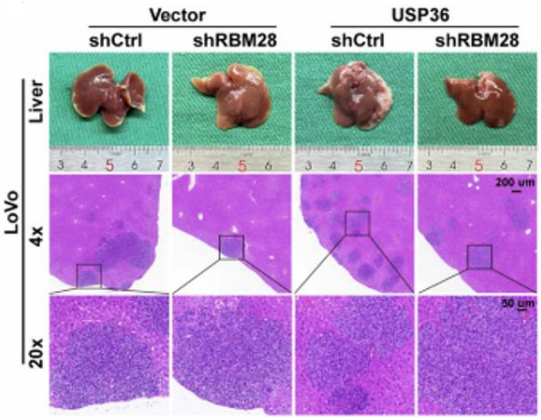

c)

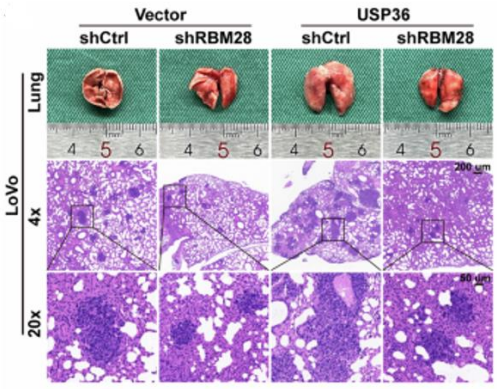

d)

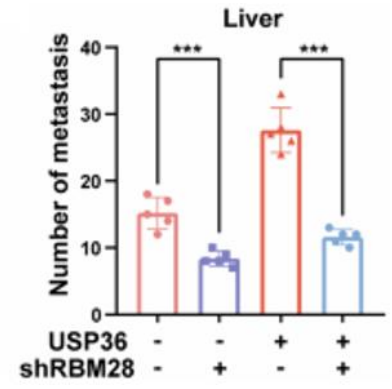

e)

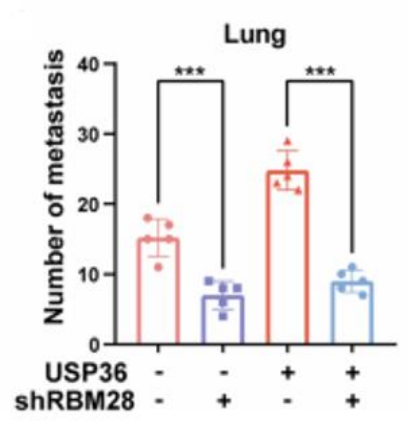

f)

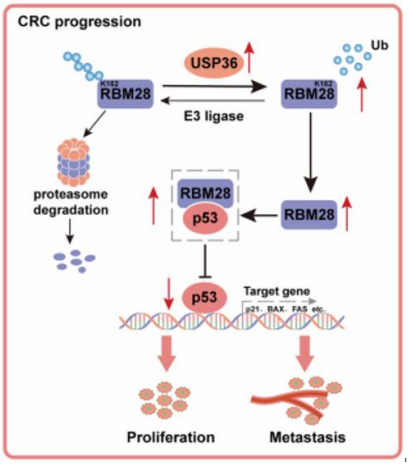

g)

Figure 8. USP36 enhances colorectal cancer cell growth and metastatic potential reliant on RBM28.

A Example images of subcutaneous tumors harvested from nude mice. Tumor dimensions were recorded every 5 days, and final masses were determined. B Hematoxylin-eosin staining and immunohistochemical analysis of xenograft sections. Ki67 levels were assessed via IHC. C–F Example photographs and H&E-stained images of metastatic lesions in mouse livers and lungs. Counts of metastatic foci in liver or lung were quantified. G Diagram illustrating the proposed mechanism of USP36 action in colorectal cancer. USP36 removes ubiquitin from RBM28 at lysine 162, thereby increasing its stability. Elevated RBM28 subsequently binds p53, blocking its transcriptional function and resulting in suppression of the p53 pathway. All results are shown as means ± SD from three separate experiments. ***p < 0.001 [8].

Subsequently, we tested if the USP36/RBM28 oncogenic actions operate via the p53 pathway. Viability and clonogenic assays revealed that the p53 activator Idasanutlin strongly reduced cell growth and abolished the proliferation boost from combined USP36 and RBM28 overexpression in LoVo cells. Apoptosis detection by flow cytometry similarly showed Idasanutlin increased cell death and countered the anti-apoptotic effect of USP36/RBM28 elevation. Moreover, Idasanutlin substantially impaired migratory and invasive capacities of LoVo cells and neutralized the enhanced metastasis promoted by USP36 and RBM28. Overall, these data confirm that the USP36/RBM28 pair drives malignant phenotypes through p53 pathway suppression and indicate Idasanutlin as a candidate to disrupt this axis in colorectal cancer cells.

Deubiquitinating enzymes (DUBs) are now widely acknowledged for contributing to tumor advancement and spread by altering various signaling cascades [12]. In this work, we identified USP36, a member of the DUB family, as a key modulator of p53 signaling in colorectal cancer. USP36 binds RBM28 and elevates its protein stability by blocking proteasomal degradation through deubiquitination. The resulting higher RBM28 forms a complex with p53, impairing p53-driven transcription and thus promoting colorectal cancer cell growth and metastatic dissemination **(Figure 8g)** [8].

So far, several substrates of USP36 have been reported, such as ALKBH5 [14], TAZ [15], YAP [16], ALR [17], Snail1 [27], and CHD7 [28]. Here, we uncovered RBM28 as a new target of USP36 in colorectal cancer. Prior reports indicated elevated RBM28 protein in multiple malignancies, including colon cancer, where it correlates with worse overall survival [26]. Silencing RBM28 reduced growth in HCT116 and U2OS lines [26]. Aligning with those findings, our data showed forced RBM28 expression accelerated colorectal cancer cell proliferation, resistance to apoptosis, invasion, and migration. In our patient samples, RBM28 was higher in tumor tissue and linked to shorter survival in high-expression cases. Furthermore, RBM28 protein amounts positively associated with USP36 in colorectal cancer specimens, suggesting USP36 controls RBM28.

Alterations in the tumor suppressor p53 occur frequently in cancers, contributing to inactivation in over 50% of cases [29, 30]. Detailed understanding of p53 regulation may reveal effective targets for colorectal cancer therapy. Earlier research described direct or indirect control of

p53 activity by various E3 ligases and DUBs, including Mdm2/Mdm4 [31, 32], TRIM28 [33], DCAF13 [34], USP42 [35], USP15 [36], among others. For example, USP7 stabilizes Mdm2 via deubiquitination, enabling Mdm2 to ubiquitinate and degrade p53 [37, 38]. USP7 can also directly deubiquitinate and protect p53 [39, 40]. The influence of USP36 on p53, however, was unknown. Our GSEA revealed a strong negative link between USP36 and p53 pathway activity. We therefore investigated USP36's potential to modulate p53, akin to other DUBs. Results showed USP36 reduces p53 promoter occupancy and downstream gene expression indirectly via RBM28, without direct binding or deubiquitination of p53 itself.

Growing data underline the importance of p53 inactivation in driving cancer proliferation and metastasis [41, 42]. This has spurred numerous trials testing p53-activating compounds [31, 43]. Idasanutlin stands out as one of the furthest advanced, now in phase III for acute myeloid leukemia [31]. Building on our results, exploring p53 activators against the USP36/RBM28/p53 cascade merits attention. We found Idasanutlin reversed the oncogenic phenotypes induced by USP36/RBM28. This positions Idasanutlin as a possible agent to interfere with USP36/RBM28-driven p53 suppression, offering a potential strategy for colorectal cancer management. Still, the ability of p53 activators to overcome USP36/RBM28-mediated p53 blockade requires additional validation in preclinical models and human trials.

Certain limitations are inherent in this investigation. First, while tissue microarray evaluation connected higher USP36 and RBM28 protein amounts to unfavorable outcomes in colorectal cancer cases, confirmation in larger patient groups remains necessary. Second, the work concentrated mainly on USP36's deubiquitination of RBM28, yet the identity of the particular E3 ubiquitin ligase responsible for RBM28 ubiquitination is still undetermined. Examining the interplay or competition between USP36 and such E3 ligases could yield greater understanding of RBM28 control mechanisms. Third, small-molecule compounds inhibiting deubiquitinases are gaining traction in oncology studies [13, 44]. Examples include IU1 against USP14 and TCID against UCHL3 [45, 46]. Regrettably, no selective inhibitors exist for USP36 at present, meriting dedicated future efforts. Finally, the scope was restricted to colorectal cancer, necessitating additional exploration of the USP36-RBM28-p53 cascade across other tumor types to broaden the impact and utility of these observations.

In conclusion, this research elucidated the critical contribution of the USP36/RBM28/p53 cascade to colorectal cancer biology. USP36 enhances RBM28 stability via deubiquitination, leading to suppression of p53 transcriptional function and consequent dampening of p53 pathway signaling. Extending from this, treatment with the p53-activating agent Idasanutlin successfully neutralized the cancer-promoting consequences of elevated USP36 and RBM28. Such evidence positions the USP36/RBM28 pathway as a candidate prognostic indicator for colorectal cancer advancement and patient survival, alongside a viable target for intervention approaches. Furthermore, the work offers useful direction for upcoming design of targeted small-molecule blockers of USP36. Achieving clinical translation and thorough comprehension of these prospects will demand extensive testing in animal models and human trials.

Materials and Methods

Clinical samples and tissue microarray construction

Surgical resection specimens from colorectal cancer individuals were obtained at the First Affiliated Hospital of Nanjing Medical University. Written informed consent was secured from every participant, and resected tissues were immediately stored at −80 °C. None of the included patients had undergone preoperative chemoradiotherapy. The tissue microarray was prepared according to prior methodology [47].

Cell culture conditions

HEK293T, HCT 116, RKO, and LoVo lines were acquired from the Type Culture Collection Cell Bank, Chinese Academy of Sciences (Shanghai, China). Cultivation occurred in DMEM/F12 medium (Biosharp, China) supplemented with 10% fetal bovine serum.

Real-time quantitative PCR (qRT-PCR)

RNA extraction employed TRIzol reagent (Invitrogen, USA) per supplier guidelines. Reverse transcription to cDNA utilized HiScript RT Mix (Vazyme, Jiangsu, China). Amplification reactions relied on the SYBR Premix Ex Taq Kit (TaKaRa Biotechnology, Dalian, China). Procedures followed established protocols from earlier work [48].

Gene silencing and expression constructs

Lentiviral particles carrying shRNAs against USP36 and RBM28 were generated by Genomeditech (Shanghai, China). Full-length coding sequences of USP36 and RBM28 from Genomeditech were inserted into lentiviral vectors. Constructs for Ub, p53, USP36, and RBM28 were also supplied by Genomeditech (Shanghai, China).

Assays for cell growth and death

Cell Counting Kit-8 and clonogenic experiments followed standard procedures [49]. Apoptosis quantification in colorectal cancer cells was performed via flow cytometry, as detailed previously [49].

Assays for motility and invasiveness

Transwell migration/invasion and scratch-wound healing tests were executed using methods outlined before [48].

Immunoblotting (Western blot)

Protein detection by Western blot adhered to routine techniques [50].

Co-immunoprecipitation (Co-IP)

Protein extracts were clarified by centrifugation at 13,000 × g for 10 min. Supernatants were incubated overnight with target-specific antibodies at 4 °C. Resulting complexes were captured on A/G magnetic beads for 1 hour at room temperature. Beads underwent two washes in IP buffer followed by one in distilled water to eliminate nonspecific interactions. Captured proteins were then analyzed by immunoblot or submitted for mass spectrometry.

GST pull-down assay

Myc-RBM28, isolated from HEK-293T cells, was incubated with GST or GST-USP36 bound to glutathione agarose beads for 2 hours at 4 °C. After incubation, the beads were washed thoroughly using GST pulldown binding buffer. Proteins retained on the beads were separated by SDS-PAGE and detected by Western blot with the indicated antibodies.

Immunofluorescence (IF)

Cells were fixed using immunostaining fixative (P0098; Beyotime), followed by blocking with blocking buffer (P0102; Beyotime) for 1 hour. Primary antibodies were applied overnight at 4 °C, and cells were then incubated with secondary antibodies for 1 hour. Nuclei were counterstained with DAPI for visualization.

Luciferase reporter assay

p53 transcriptional activity was measured using the pp53-TA-luc reporter (Beyotime Biotechnology) and the Dual-Luciferase Reporter Assay Kit (Promega, USA), following previously established protocols [47].

Chromatin immunoprecipitation (ChIP) assay

ChIP experiments were performed according to the instructions of the ChIP Kit (#56383, CST).

Ubiquitination assay

Cells were treated with MG132 (Beyotime, Shanghai, China) for 6 hours before collection. Protein extracts were subjected to Co-IP using the Myc antibody, and ubiquitinated species were detected using an HA antibody.

Immunohistochemistry (IHC)

IHC staining was performed according to standard procedures [47].

Animal experiments

Five-week-old male BALB/c nude mice were used to generate xenograft and metastasis models. For xenografts, 1 × 10^6 lentivirus-transfected CRC cells in PBS were injected subcutaneously into both axillae. Tumor size was monitored every 5 days, and mice were euthanized 25 days post-injection. Tumors were collected for weight measurement, H&E staining, and IHC analysis. For metastasis studies, 1 × 10^6 CRC cells were injected into the distal spleen or tail vein. Five weeks later, mice were injected intraperitoneally with D-luciferin (150 mg/kg; Goldbio, USA), and metastases were imaged using the IVIS 100 system (Xenogen, USA). Livers and lungs were harvested for H&E staining. All animal procedures were approved by the Ethics Committee of Nanjing Medical University (IACUC-2310047).

Statistical analysis

Data analysis was performed using GraphPad Prism 9.0 (GraphPad, La Jolla, USA). Statistical evaluations included Student's t-test, ANOVA, Pearson correlation, chi-square test, and Kaplan–Meier survival analysis. All experiments were repeated independently at least three times. Data are reported as mean ± SD, and a p-value < 0.05 was considered statistically significant.

Acknowledgments: We would like to thank the Core Facility of Jiangsu Provincial People's Hospital for its help in the detection of experimental samples.

Conflict of Interest: None

Financial Support: This work was supported by the National Natural Science Foundation (Grant Numbers 82273406, 82304221); Nature Key Research and Development Program of Jiangsu Province (BE2021742); Basic Research Program of Jiangsu Province (BK20221415, BK20230730); and Jiangsu Key Medical Discipline (General Surgery; Grant No. ZDXK202222).

Ethics Statement: Approval from the ethics committee of The First School of Clinical Medicine, Nanjing Medical University was obtained for the human tissue study, and informed consent was provided by all patients involved. All animal experiments are conducted with the approval of the Committee on the Ethics of Animal Experiments of Nanjing Medical University. The ethical number of the animal experiment is IACUC-2310047. All methods were performed in accordance with the relevant guidelines and regulations.

References

1. Siegel RL, Giaquinto AN, Jemal A. Cancer statistics, 2024. CA Cancer J Clin. 2024;74:12–49.
2. Dekker E, Tanis PJ, Vleugels JLA, Kasi PM, Wallace MB. Colorectal cancer. Lancet. 2019;394:1467–80.
3. Cassidy S, Syed BA. Colorectal cancer drugs market. Nat Rev Drug Discov. 2017;16:525–6.
4. Swatek KN, Komander D. Ubiquitin modifications. Cell Res. 2016;26:399–422.
5. Kleiger G, Mayor T. Perilous journey: a tour of the ubiquitin-proteasome system. Trends Cell Biol. 2014;24:352–9.
6. Cruz Walma DA, Chen Z, Bullock AN, Yamada KM. Ubiquitin ligases: guardians of mammalian development. Nat Rev Mol Cell Biol. 2022;23:350–67.
7. Qi J, Ronai ZeA. Dysregulation of ubiquitin ligases in cancer. Drug Resist Updat. 2015;23:1–11.
8. Popovic D, Vucic D, Dikic I. Ubiquitination in disease pathogenesis and treatment. Nat Med. 2014;20:1242–53.
9. Rape M. Ubiquitylation at the crossroads of development and disease. Nat Rev Mol Cell Biol. 2018;19:59–70.
10. Song L, Luo Z-Q. Post-translational regulation of ubiquitin signaling. J Cell Biol. 2019;218:1776–86.
11. Komander D, Clague MJ, Urbé S. Breaking the chains: structure and function of the deubiquitinases. Nat Rev Mol Cell Biol. 2009;10:550–63.
12. Dewson G, Eichhorn PJA, Komander D. Deubiquitinases in cancer. Nat Rev Cancer. 2023;23:842–62.
13. Harrigan JA, Jacq X, Martin NM, Jackson SP. Deubiquitylating enzymes and drug discovery: emerging opportunities. Nat Rev Drug Discov. 2018;17:57–78.
14. Chang G, Xie GS, Ma L, Li P, Li L, Richard HT. USP36 promotes tumorigenesis and drug sensitivity of glioblastoma by deubiquitinating and stabilizing ALKBH5. Neuro Oncol. 2023;25:841–53.
15. Wang D, Li Z, Li X, Yan C, Yang H, Zhuang T, et al. DUB1 suppresses Hippo signaling by modulating TAZ protein expression in gastric cancer. J Exp Clin Cancer Res. 2022;41:219.
16. Zhang W, Luo J, Xiao Z, Zang Y, Li X, Zhou Y, et al. USP36 facilitates esophageal squamous carcinoma progression via stabilizing YAP. Cell Death Dis. 2022;13:1021.
17. Zheng M, Ai Z, Guo Y, Chen Y, Xie P, An W. Imbalance in ALR ubiquitination accelerates the progression of nonalcoholic steatohepatitis to hepatocellular carcinoma. Oncogene. 2023;42:308–21.
18. Hernández Borrero LJ, El-Deiry WS. Tumor suppressor p53: biology, signaling pathways, and therapeutic targeting. Biochim Biophys Acta Rev Cancer. 2021;1876:188556.
19. Wang M, Attardi LD. A balancing act: p53 activity from tumor suppression to pathology and therapeutic implications. Annu Rev Pathol. 2022;17:205–26.
20. Powell E, Piwnica-Worms D, Piwnica-Worms H. Contribution of p53 to metastasis. Cancer Discov. 2014;4:405–14.
21. Boutelle AM, Attardi LD. p53 and tumor suppression: it takes a network. Trends Cell Biol. 2021;31:298–310.
22. Thomas AF, Kelly GL, Strasser A. Of the many cellular responses activated by TP53, which ones are critical for tumour suppression? Cell Death Differ. 2022;29:961–71.

23. Hassin O, Oren M. Drugging p53 in cancer: one protein, many targets. Nat Rev Drug Discov. 2023;22:127–44.
24. Best MG, Sol N, In T Veld SGJG, Vancura A, Muller M, Niemeijer AN, et al. Swarm intelligence-enhanced detection of non-small-cell lung cancer using tumor-educated platelets. Cancer Cell. 2017;32:238–252.e9.
25. Sebestyén E, Singh B, Miñana B, Pagès A, Mateo F, Pujana MA, et al. Large-scale analysis of genome and transcriptome alterations in multiple tumors unveils novel cancer-relevant splicing networks. Genome Res. 2016;26:732–44.
26. Lin X, Zhou L, Zhong J, Zhong L, Zhang R, Kang T, et al. RNA-binding protein RBM28 can translocate from the nucleolus to the nucleoplasm to inhibit the transcriptional activity of p53. J Biol Chem. 2022;298:101524.
27. Qin K, Yu S, Liu Y, Guo R, Guo S, Fei J, et al. USP36 stabilizes nucleolar Snail1 to promote ribosome biogenesis and cancer cell survival upon ribotoxic stress. Nat Commun. 2023;14:6473.
28. Mondal T, Juvvuna PK, Kirkeby A, Mitra S, Kosalai ST, Traxler L, et al. Sense-antisense lncRNA pair encoded by locus 6p22.3 determines neuroblastoma susceptibility via the USP36-CHD7-SOX9 regulatory axis. Cancer Cell. 2018;33:417–434.e7.
29. Vousden KH, Prives C. Blinded by the light: the growing complexity of p53. Cell. 2009;137:413–31.
30. Vogelstein B, Lane D, Levine AJ. Surfing the p53 network. Nature. 2000;408:307–10.
31. Duffy MJ, Synnott NC, O'Grady S, Crown J. Targeting p53 for the treatment of cancer. Semin Cancer Biol. 2022;79:58–67.
32. Huang J. Current developments of targeting the p53 signaling pathway for cancer treatment. Pharmacol Ther. 2021;220:107720.
33. Jin J-O, Lee GD, Nam SH, Lee TH, Kang DH, Yun JK, et al. Sequential ubiquitination of p53 by TRIM28, RLIM, and MDM2 in lung tumorigenesis. Cell Death Differ. 2021;28:1790–803.
34. Wei S, Xing J, Chen J, Chen L, Lv J, Chen X, et al. DCAF13 inhibits the p53 signaling pathway by promoting p53 ubiquitination modification in lung adenocarcinoma. J Exp Clin Cancer Res. 2024;43:3.
35. 35.Hock AK, Vigneron AM, Carter S, Ludwig RL, Vousden KH. Regulation of p53 stability and function by the deubiquitinating enzyme USP42. EMBO J. 2011;30:4921–30.
36. Zou Q, Jin J, Hu H, Li HS, Romano S, Xiao Y, et al. USP15 stabilizes MDM2 to mediate cancer-cell survival and inhibit antitumor T cell responses. Nat Immunol. 2014;15:562–70.
37. Cummins JM, Rago C, Kohli M, Kinzler KW, Lengauer C, Vogelstein B. Tumour suppression: disruption of HAUSP gene stabilizes p53. Nature. 2004;428:1.
38. Cummins JM, Vogelstein B. HAUSP is required for p53 destabilization. Cell Cycle. 2004;3:689–92.
39. Li M, Brooks CL, Kon N, Gu W. A dynamic role of HAUSP in the p53-Mdm2 pathway. Mol Cell. 2004;13:879–86.
40. Li M, Chen D, Shiloh A, Luo J, Nikolaev AY, Qin J, et al. Deubiquitination of p53 by HAUSP is an important pathway for p53 stabilization. Nature. 2002;416:648–53.
41. Solé L, Lobo-Jarne T, Álvarez-Villanueva D, Alonso-Marañón J, Guillén Y, Guix M, et al. p53 wild-type colorectal cancer cells that express a fetal gene signature are associated with metastasis and poor prognosis. Nat Commun. 2022;13:2866.
42. Liu Y, Su Z, Tavana O, Gu W. Understanding the complexity of p53 in a new era of tumor suppression. Cancer Cell. 2024;42:946–67.
43. Peuget S, Zhou X, Selivanova G. Translating p53-based therapies for cancer into the clinic. Nat Rev Cancer. 2024;24:192–215.
44. Deng L, Meng T, Chen L, Wei W, Wang P. The role of ubiquitination in tumorigenesis and targeted drug discovery. Signal Transduct Target Ther. 2020;5:11.
45. Wang Y, Jiang Y, Ding S, Li J, Song N, Ren Y, et al. Small molecule inhibitors reveal allosteric regulation of USP14 via steric blockade. Cell Res. 2018;28:1186–94.
46. Ouyang L, Yan B, Liu Y, Mao C, Wang M, Liu N, et al. The deubiquitylase UCHL3 maintains cancer stem-like properties by stabilizing the aryl hydrocarbon receptor. Signal Transduct Target Ther. 2020;5:78.
47. Jin C, Wang T, Zhang D, Yang P, Zhang C, Peng W, et al. Acetyltransferase NAT10 regulates the Wnt/β-catenin signaling pathway to promote colorectal cancer progression via ac4C acetylation of KIF23 mRNA. J Exp Clin Cancer Res. 2022;41:345.
48. Peng C, Tan Y, Yang P, Jin K, Zhang C, Peng W, et al. Circ-GALNT16 restrains colorectal cancer progression by enhancing the SUMOylation of hnRNPK. J Exp Clin Cancer Res. 2021;40:272.

49. Zhou J, Wang L, Sun Q, Chen R, Zhang C, Yang P, et al. Hsa_circ_0001666 suppresses the progression of colorectal cancer through the miR-576-5p/PCDH10 axis. Clin Transl Med. 2021;11:e565.

50. Yang P, Li J, Peng C, Tan Y, Chen R, Peng W, et al. TCONS_00012883 promotes proliferation and metastasis via DDX3/YY1/MMP1/PI3K-AKT axis in colorectal cancer. Clin Transl Med. 2020;10:e211.